

# Electron transport in quasi-ballistic FETs subjected to a magnetic field

M. Yeliseiev<sup>1, a)</sup> and V. A. Kochelap<sup>1, 2</sup>

<sup>1)</sup>*Institute of Semiconductor Physics, National Academy of Sciences of Ukraine, Kyiv 03028, Ukraine;*

<sup>2)</sup>*Institute of High Pressure Physics, Polish Academy of Sciences, Warsaw 01-142, Poland*

We report the study of quasi-ballistic electron transport in short FETs subjected to magnetic field. Spatial distributions of electron concentrations, velocities, Hall currents and voltages in the short FET channels are determined. The basic properties of current-voltage characteristics of quasi-ballistic FETs in magnetic field are analyzed, among these the kink-like characteristics of the near-ballistic device. Peculiarities of magnetoresistance of such FETs are studied for low and high magnetic fields, and different current regimes. For nonlinear current regimes we revealed significantly larger magnetoresistance for the devices with higher ballisticity. Numerical estimates of studied effects are presented. We suggest, that the found results contribute to the physics of short FETs and can be used for developing nanoscale devices for particular applications.

## I. INTRODUCTION

In semiconductor structures and devices with short (submicron) conductive channels electrons experience only a few scatterings by defects and phonons during time of their transit through the devices. Physics of these ballistic or quasi-ballistic electron transport regimes is distinctly different from that of essentially dissipative (drift-diffusion) regimes characteristic for microscale devices. Examples of new effects emerging in near-ballistic device regimes include both quantum<sup>1</sup> and semiclassical phenomena. Among the latter we may cite velocity overshoot,<sup>1</sup> manifestation of nonparabolic energy dispersion,<sup>3</sup> run-away effect,<sup>2</sup> excitation of plasmonic resonances,<sup>4,5</sup> a large effect of lattice vibrations on the ultrahigh frequency transport in polar materials,<sup>6,7</sup> etc. Exploitation of these phenomena may open a way to new classes of nanoelectronic and optoelectronic devices.

Of nanoscale devices, field effect transistors (FETs) with short active channels hold an important position because of interesting physics and numerous areas of their applications. A great number of papers was dedicated to experimental and theoretical studies of these nanoscale devices (see, for example, [8–10]). Particularly, in the focus of attention were and remain spatial distributions and temporal dependencies of electric potentials, charge carriers (primary theoretical studies) and kinetic characteristics of the carriers, etc. Additional information on key characteristics in small sized FETs can be obtained by using magnetic field, which affects carrier motion. Experimental measurements for small sizes FETs in magnetic fields transverse to electron transport were reported in papers,<sup>12–14</sup> where the authors have used the theory of dissipative galvanomagnetic transport. However, in ballistic and quasi-ballistic transport regimes, influence of magnetic fields is different from that for essentially dissipative transport<sup>11</sup> and requires additional investigation.

*Pure ballistic* FETs in magnetic fields were consid-

ered in paper,<sup>15</sup> where unusual distributions of electron concentration and velocity, and kink-like current-voltage characteristics were predicted. In the present paper, we analyze peculiarities of carrier transport and properties of *quasi-ballistic* FETs subjected to a magnetic field. This facilitates understanding of behavior of such FETs at actual momentum dissipation of electrons and can be used for developing nanoscale devices for particular applications.

## II. BASIC ASSUMPTIONS AND EQUATIONS

It has long been known that, result of action of transverse magnetic fields on electron transport (the Hall effect) strongly depends on specimen geometry and patterns of current/electric field.<sup>16,17</sup> For a rectangular specimen with length  $L$  along the current and width  $W$  transverse to the current, the Hall electric field/voltage builds up if  $L \gg W$ , then no transverse current and magnetoresistance arise for this case. In recent paper<sup>18</sup> for a specially designed gated structure with  $L \gg W$ , the Hall voltage was studied in detail for linear and nonlinear transport regimes. In opposite case  $L \ll W$ , which is typical for FETs geometry,<sup>19</sup> the Hall field/voltage is shortened by source and drain contacts. Instead, both transverse Hall current and magnetoresistance appear. Below we will consider FETs of this geometry.

We will use the Dyakonov-Shur model, for which the electron transport is considered as a charged fluid confined in a narrow layer and governed by hydrodynamic equations.<sup>20</sup> The electrons are characterized by the area density,  $n$ , and by the velocity,  $\mathbf{v} = \{v_x, v_y\}$ , induced by source-drain electric bias,  $\phi$ , and a transverse magnetic field,  $H_z = H$ . For the above assumed geometry of FET, we can consider that all quantities  $n$ ,  $\mathbf{v}$ ,  $\phi$  are dependent only on coordinate along source-drain direction,  $x$ . In the frame of the gradual channel approximation<sup>1,21</sup>, the local potential is supposed to be proportional to the electron density. The complete system of equations for this

<sup>a)</sup>Electronic mail: mykola.eliseev@gmail.com

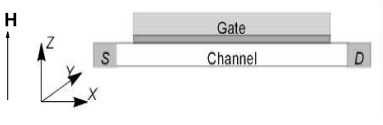


FIG. 1. A sketch of FET under consideration.

model of quasi-ballistic FET reads:

$$\frac{\partial v_x}{\partial t} + v_x \frac{\partial v_x}{\partial x} + \frac{v_x}{\tau} = \frac{e}{m} \frac{\partial \phi(x, h)}{\partial x} - \frac{e}{cm} v_y H, \quad (1)$$

$$\frac{\partial v_y}{\partial t} + v_x \frac{\partial v_y}{\partial x} + \frac{v_y}{\tau} = \frac{e}{cm} v_x H, \quad (2)$$

$$\frac{\partial n}{\partial t} + \frac{\partial j_x}{\partial x} = 0, \quad j_x = n v_x, \quad (3)$$

$$\phi(x, z) = -\frac{4\pi e}{\kappa} n(x) z + \phi_g \quad (0 \leq z \leq h). \quad (4)$$

These equations are for the frame of reference presented in Fig. 1, where geometry parameters of the FET under consideration are indicated; the conductive layer and the gate are situated at  $z = h$  and  $z = 0$ , respectively. The voltage applied to the gate is  $\phi_g$ ;  $m$  and  $-e$  are the electron effective mass and the electron charge,  $\kappa$  is the dielectric constant,  $\tau$  is an electron relaxation time,  $c$  is the light velocity, the last terms in Eqs. (1) and (2) are projections of the Lorentz force;  $j_x$  is the electron source-drain flux density. Eq. (3) obtained for the gradual channel approximation is valid at  $L \gg h$  and characteristic scale of  $\phi(x)$  variation is much larger than  $h$ .

### III. THE STEADY-STATE SOLUTIONS

For the steady-state, Eq. (3) gives for the electron flux density:  $j_x = n v_x = j_0$  with  $j_0$  being an integration constant. It is convenient to solve the system (1)-(4) at a given  $j_0$  and then to find the voltage drop on the device,  $\phi(L)$  and other characteristics. The boundary conditions for Eq. (1), (2) are  $v_x(0) = j_0/n_s$  and  $v_y(0) = 0$ , with  $n_s = n(0)$  being the electron area density near the source. For what follows, we introduce dimensionless variables and parameters:

$$\xi = \frac{x}{L}, \quad V_{x,y} = \frac{v_{x,y}}{v_s}, \quad N := \frac{n}{n_s}, \quad J_x = \frac{j_0}{j_{sc}}, \quad (5)$$

$$\Phi(\xi) = \frac{[\phi(\xi, -h) - \phi_g]}{u_{sc}}, \quad u_{sc} = \frac{4\pi e h n_s}{\kappa}, \quad (6)$$

$$j_{sc} = \sqrt{\frac{4\pi e^2 h n_s^3}{m \kappa}}, \quad \mathcal{B} = \frac{L}{\tau v_p}, \quad v_p = \sqrt{\frac{4\pi e^2 h n_s}{m \kappa}}, \quad (7)$$

$$\Omega = \omega_c \tau, \quad \Omega' = \omega_c \frac{L}{v_p}, \quad \omega_c = \frac{e}{cm} H. \quad (8)$$

Here the scaling parameters for the flux,  $j_{sc}$ , and the potential,  $u_{sc}$ , account for the effect of interaction of the electrons with the metal gate. Note, in these notations,

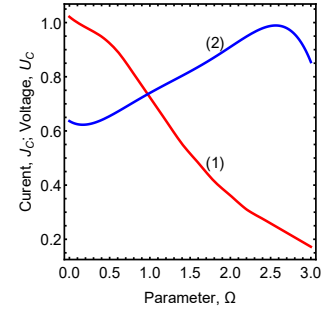


FIG. 2. Critical dimensionless currents,  $J_c$  (scaled to their values at  $\Omega = 0$ ) and voltages,  $U_c$  as functions of dimensionless magnetic field,  $\Omega$ .

dimensionless voltage drop on the conductive channel is  $U = \Phi(1) - \Phi(0) = N(0) - N(1) \equiv 1 - N(1)$ . Factor  $\mathcal{B}$  is the only parameter dependent on kinetic characteristic, which is the electron relaxation time,  $\tau$ ;  $\omega_c$  is the cyclotron frequency. For the quasi-ballistic regime, it is convenient to characterize the magnetic field by the dimensional cyclotron frequency,  $\Omega$ . Parameter  $v_p$  is known as the velocity of gated plasmons<sup>4,5</sup>; it becomes especially important parameter for near-ballistic regime with  $\tau \gg \tau_{tr}$ ,  $\tau_{tr} = L/v_p$ , i.e.,  $\mathcal{B} \ll 1$ . For the latter regime, the characteristic time is the transit time,  $\tau_{tr}$ , and relevant dimensional cyclotron frequency is  $\Omega'$ .

For the steady-state problem at a given electron flux/current,  $J_x$ , dimensionless electron concentration,  $N(\xi)$ , and velocity,  $V_x(\xi)$ , are related through equation  $N(\xi) V_x(\xi) = 1$ . Then, accepting notations (5)-(8) the dynamic equations (1), (2) can be rewritten in terms  $N(\xi)$ ,  $V_y(\xi)$ :

$$\frac{dN}{d\xi} = \frac{\mathcal{B} J_x N^2}{J_x^2 - N^3} (1 + \Omega N V_y), \quad (9)$$

$$\frac{dV_y}{d\xi} = \frac{\mathcal{B}}{J_x} (-N V_y + \Omega), \quad (10)$$

with boundary conditions at the cathode side  $N(0) = 1$ ,  $V_y(0) = 0$ .

Two general conclusions immediately follow from this system of equations. First, reasonable solutions<sup>22</sup> exist only at  $J_x < 1$  (see discussion below). Second, the first integral of equations can be found in an explicit form:

$$\Omega J_x^2 V_y + J_x^2 \frac{N-1}{N} + \frac{1-N^2}{2} = \mathcal{B} J_x (1 + \Omega^2) \xi. \quad (11)$$

This relationship allows to find the equation of the first order for  $N(\xi)$  and facilitates determination of  $V_y(\xi)$  and the Hall current density  $J_y(\xi)$ , when the dependence  $N(\xi)$  will be found. The basic Eqs. (9), (10) contain a given current density  $J_x$  and two parameter:  $\mathcal{B}$ , which as easy to find is dimensionless FET resistance density, and  $\Omega \propto H$ . At that, the product  $\mathcal{B} \Omega$  does not depend on the relaxation time. The case  $\mathcal{B} \ll 1$  corresponds to nearly ballistic electron transport. The opposite case,

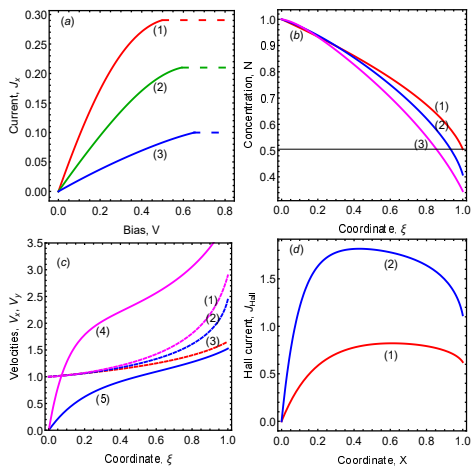


FIG. 3. Results of calculations of quasi-ballistic FET in magnetic fields with  $\mathcal{B} = 1$ . (a): The dimensionless current-voltage characteristics. (b): Spatial distributions of the electron concentration,  $N(\xi)$ . (c): Distributions of electron velocities,  $V_x(\xi)$ ,  $V_y(\xi)$ . (d): Distributions of the Hall current densities,  $J_y(\xi)$ . In (a), (b) and (c) curves 1, 2, 3 for  $\Omega = 0, 1, 2$ , respectively. In (c) curves 1 - 3 for  $V_x(\xi)$ ; curves 4, 5 for  $V_y(\xi)$  at  $\Omega = 1, 2$ . In (d) curves 1, 2 for the Hall current densities. Results in (b)-(d) are given for critical currents given in the text.

$\mathcal{B} \gg 1$ , is relevant to dissipative transport. The general property of the Dyakonov-Shur model and Eqs. (9), (10) is the existence of physically reasonable solutions only in some interval of currents,  $[0, J_c]$  and corresponding voltage drop interval  $[0, U_c]$ , with the critical values  $J_c$  and  $U_c$  dependent on  $\mathcal{B}$  and the magnetic field magnitude,  $H$ . At approaching the critical voltage,  $U \rightarrow U_c$  the current has a tendency to saturate. Dependencies of the critical values,  $J_c, U_c$  on the magnetic field is shown in Fig. 2. Note, in quasi-ballistic FETs actually there is no pinching-off of the conductive channel. The real pinch-off effect arises at large  $\mathcal{B}$  (at strongly dissipative transport). Instead, the electric field in the channel diverges near the drain contact for the limit  $J \rightarrow J_c$ .

In Fig. 3 (a) we present the current-voltage characteristic for quasi-ballistic FET with  $\mathcal{B} = 1$ , i.e., the case of moderate relaxation. Saturation portions of  $J - U$  dependencies are shown conditionally. As seen, the magnetic field suppresses source-drain current, decreases its critical value,  $J_c$ , and increases critical voltage,  $U_c$ :  $J_c \approx 0.29, U_c \approx 0.6$  at  $\Omega = 0$ ;  $J_c \approx 0.21, U_c \approx 0.68$ ;  $\Omega = 1, J_c \approx 0.1, U_c \approx 0.77$  at  $\Omega = 2$ . Corresponding spatial distributions of the electron concentration are given in Fig. 3 (b), which evidences that magnetic field induces more rapid decrease of the concentration along the channel. Magnetic field also leads to an increase of the electron velocity along the channel,  $V_x(\xi)$ , and generates transverse velocity,  $V_y(\xi)$ , which can exceed  $V_x$  at high magnetic fields, as seen from Fig. 3 (c). Higher velocities of the electrons,  $V_x, V_y$ , are achieved for the expense of larger voltage drop in the presence of magnetic field. The

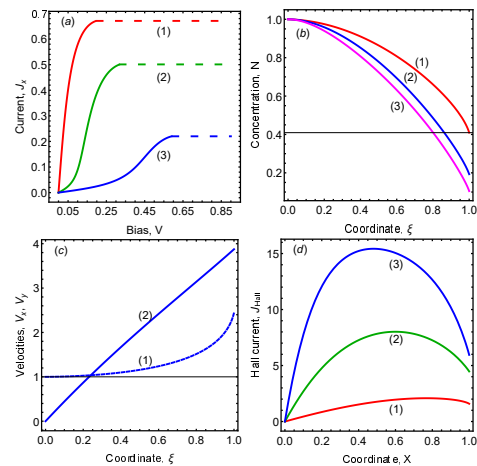


FIG. 4. Results of calculations of near-ballistic FET in magnetic fields with  $\mathcal{B} = 0.1$ . (a): The dimensionless current-voltage characteristics. (b): Spatial distributions of the electron concentration,  $N(\xi)$ . (c): Distributions of electron velocities,  $V_x(\xi)$ ,  $V_y(\xi)$ . (d): Distributions of the Hall current densities,  $J_y(\xi)$ . In (a), (b) curves 1 - 4 for  $\Omega' = 1, 1.5, 2$ , respectively. In (c) curves 1, 2 for  $V_x(\xi)$  at  $\Omega' = 1$ ; . In (d) curves 1, 2, 3 for the Hall current densities at  $\Omega' = 1, 1.5, 2$ . Results in (b), (c), (d) are given for critical currents given in the text.

Hall current densities,  $J_h = V_y(\xi)N(\xi)$ , are nonuniform, they are shown in Fig. 3 (d) for  $\Omega = 1, 2$ . The total Hall currents,  $I_H = \int_0^1 d\xi J_H(\xi)$ , for the presented distributions are  $I_H = 0.67$  and  $1.56$ , respectively (while total source-drain currents in the FET should be estimated as  $I_{sd} = J_x W/L$ ).

#### IV. THE NEAR-BALLISTIC REGIME

As seen from the Fig. 3 (a), for quasi-ballistic transport regime ( $\mathcal{B} \gtrsim 1$ ) the current-voltage characteristics have the form typical for FETs.<sup>19,21</sup> Situation changes cardinally for the *near-ballistic* transport regime, when  $\mathcal{B} \ll 1$ . In Fig. 4 we present the current-voltage characteristics calculated at  $\mathcal{B} = 0.1$ , that corresponds to 10 times increase in the relaxation time,  $\tau$ , comparing the results in Fig. 3. To keep amplitudes of the magnetic field the same, as above, we used the parameter  $\Omega' = \mathcal{B}\Omega$ , that does not dependent on  $\tau$  and is more adequate characteristic of the  $H$ -field for near-ballistic regime (see Eqs. (8)). One can see, that the magnetic field not only suppresses the currents, but strongly increases the critical currents/voltages and modifies the  $J - U$  dependence toward unusual kink-like shape with an inflection point and two successive portions of this dependence with positive and negative curvatures.

The origin of such a behavior of the  $J - U$  characteristic can be understood by considering the *pure ballistic* limit of the electron transport. First, we should mention that in the absence of magnetic field the Dyakonov-Shur

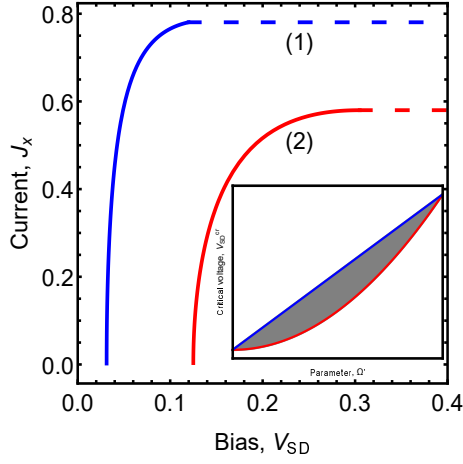


FIG. 5. Pure ballistic FET in magnetic field. Main panel -  $J - U$ -characteristics for  $\Omega' = 0.3$  and  $0.54$ . Inset: region of existing solutions of Eq. (12) in the  $\{U, \Omega'\}$ -plane.

model has no solutions for this limiting regime. For a finite value of the magnetic field, i.e., finite  $\Omega$ , setting  $\mathcal{B} = 0$  in Eqs. (9) - (11), we find following implicit expression for  $N(\xi)$  at a given  $J$ :

$$1 - N(\xi) - J^2 \frac{1 - N(\xi)^2}{2N(\xi)^2} = \frac{1}{2} \Omega'^2 \xi^2. \quad (12)$$

Using this equation for  $\xi = 1$ , we find that the electron transport arises at finite threshold voltage  $U_{th} = \Omega'^2/2 < 1$  with small, square root dependent current above the threshold:

$$J = \sqrt{\frac{2(U - U_{th})}{U_{tr}(2 - U_{tr})}} (1 - U_{tr}).$$

Existence of a threshold for the current, absence of a linear portion of  $J - U$ -characteristic and its negative curvature explain the kink-like behavior of this dependence. Arising strongly nonlinear resistance of the device is not related to conventional dissipative processes. Instead, it arises due to pump over electric energy into the Hall currents. Indeed, calculations indicate that the Hall velocity increases much faster than the velocity in the source-to-drain direction. From Eq. (12) it follows that the source-drain currents occur in a finite over-threshold interval of the voltage,  $U$ , with a tendency of suppression of the current values, when the magnetic field increases. At high magnetic fields ( $\Omega' > \sqrt{2}$ ), solutions of Eq. (12) and the currents are absent. In the inset to Fig. 5, the region of existing solutions to Eq. (12) is shown in the  $\{U, \Omega'\}$ -plane. In the main panel of this figure, examples of  $J - U$ -characteristics for the pure ballistic regime are presented.

Consideration of even small electron dissipation restores the currents in the sub-threshold voltage range, as demonstrated in Fig. 4 (a). Results in Fig 4 (b) show that in the near-ballistic regime the concentration decreases faster along the channel and the total voltage

drop are larger comparing to the quasi-ballistic regime (see Fig. 3 a). This, particularly, corresponds to larger electric fields acting the electrons. Faster growth of the Hall velocity,  $V_y$ , in comparison with the velocity  $V_x$  is illustrated in Fig. 4 (c). This explains high values of the Hall current densities, as demonstrated in Fig. 4 (d). Respective total Hall currents are  $I_H = 0.57, 2.39$  and  $5.6$  at  $\Omega' = 1, 1.5$  and  $2$ , respectively.

## V. MAGNETORESISTANCE AT ARBITRARY CURRENTS

Dimensionless FET resistance in nonlinear current regime can be defined as

$$R = \frac{U}{J} = \frac{1 - N(1)}{J}. \quad (13)$$

Thus, dependence of the electron concentration at the drain side,  $N(1)$ , on magnetic field directly gives the magnetic resistance of the FET. Note, in the absence of the  $H$ -field for the linear regime (small  $U$  and  $J$ )  $R = R_0 = \mathcal{B}$ .

In the case of small magnetic field, the magnetoresistance for arbitrary currents can be calculated as follows. Considering in Eqs. (9), (10) terms proportional to  $\Omega$  as small, we find the solution of Eq. (10) in the form

$$V_y(\xi) = \frac{\mathcal{B} \Omega}{J_0} \int_0^\xi d\xi' e^{\frac{\mathcal{B}}{J_0} [f^{\xi'} dx' N_0(x') - f^\xi dx N_0(x)]}, \quad (14)$$

where  $J_0 \equiv J_x$  and  $N_0(\xi)$  are the current and electron concentration in the absence of the  $H$ -field. From Eq. (9), we obtain perturbation of the electron concentration,  $N_1(\xi)$ :

$$N_1(\xi) = \frac{\mathcal{B}^2 \Omega^2 (N_0(\xi))^2}{J_0^2 - (N_0(\xi))^2} \times \int_0^\xi d\xi' N_0(\xi') \int_0^{\xi'} d\xi'' e^{\frac{\mathcal{B}}{J_0} [f^{\xi''} dx' N_0(x') - f^{\xi'} dx N_0(x)]}. \quad (15)$$

Dependence  $N_0(\xi)$  in the implicit form is given by the relationship (11) at  $\Omega = 0$ . Eq. (15) shows that always  $N_1(\xi) < 0$  and proportional to  $\Omega^2$ . Thus, for small magnetic fields the FET magnetoresistance,  $\Delta R = -N_1(1)/J_0$ , is positive and quadratic in the  $H$  field.

Eq. (15) can be rewritten to the form dependent only of the voltage drop,  $U_0$  and respective current  $J_0$ . Indeed, from Eq. (9) at  $\Omega = 0$  it follows, that

$$d\xi = \frac{J_0^2 - (N_0(\xi))^3}{\mathcal{B} J_0 N_0^2(\xi)} dN_0.$$

Thus in Eq. (15) we can change integrations over  $\xi'$ ,  $\xi''$  by integrations over  $N'$ ,  $N''$ . The result gives the follow-

ing closed form for the magnetoresistance:

$$\Delta R = \Omega^2 \frac{(1-U_0)^2}{J_0^2[(1-U_0)^3 - J_0^2]} \int_1^{(1-U_0)} \frac{dN}{N} [J_0^2 - N^3] \times \int_1^N \frac{dN'}{N'^2} [J_0^2 - N'^3] e^{[P(N') - P(N)]} \quad (16)$$

with

$$P(N) = \frac{\mathcal{B}}{J_0} \int_1^N \frac{dN'}{N'^2} [J_0^2 - N'^3].$$

Eq. (16) allows to find the magnetoresistance at small magnetic fields for both linear and nonlinear current/voltage regimes. In Fig. 6 (a) we present the factor  $\Delta R/\Omega^2$  for different values of dimensionless FET resistance at small biases,  $\mathcal{B}$ . One can see that the magnetoresistance increases in the nonlinear current regime with the tendency to divergence approaching critical currents/biases. Furthermore, while at low bias the magnetoresistance is larger for more dissipative channels ( $\mathcal{B}$  is larger), for the nonlinear regime, in opposite, this resistance is larger for channels with larger ballisticsity ( $\mathcal{B}$  is smaller).

At large magnetic fields, the FET resistance is presented in Figs. 6 (b), (c) as a function of  $\Omega$  for different values of the current. The resistance was calculated as follows. For a given  $\Omega$ , we find the  $J-U$ -characteristic. Then, at a fixed  $J < J_c$  the voltage drop  $U$  can be determined and  $R$  is calculated according to Eq. (13). In panels (b) and (c) the results are given for quasi-ballistic ( $\mathcal{B} = 1$ ) and near-ballistic ( $\mathcal{B} = 0.1$ ) FETs, respectively. For the latter case the magnetoresistance is considerably larger despite smaller electron dissipation. When current changes, sequences of the curves  $R(\Omega)$  are opposite for these two transport regimes, as indicated in Figs. 6 (b), (c).

## VI. NUMERICAL ESTIMATES

The above results presented in the dimensional form can be applied to analyze quasi-ballistic FETs made of different materials and with different geometry parameters. For that the scaling parameters of voltage,  $u_{sc}$ , current,  $j_{sc}$ , velocity,  $v_p$ , as well as parameter  $\mathcal{B}$ , have to be estimated. The scaling parameters are determined by the electron characteristics, charge, mass, area concentration, and dielectric surrounding and distance between the channel and the gate,  $h$ . These parameters reflect the essentiality of electron-metal gate interaction. The parameter  $\mathcal{B}$  also depends on the electro relaxation time,  $\tau$ , and the channel length  $L$ .

For numerical estimates, we consider the FET with the GaAs conductive channel. We set  $m = 0.063 m_0$ ,  $\kappa = 10.9$ ,  $n_s = 10^{12} \text{ cm}^{-2}$  and  $h = 5 \times 10^{-7} \text{ cm}$ . Then, the scaling parameters for voltage, current density and velocity are  $u_{sc} = 83 \text{ mV}$ ,  $e j_{sc} = 7.3 \text{ A/cm}$  and  $v_p =$

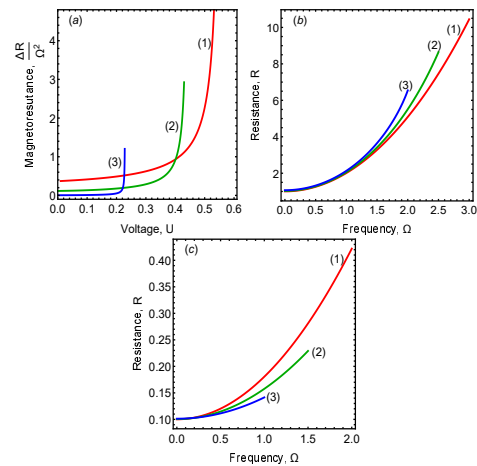


FIG. 6. (a): Factor  $\Delta R/\Omega^2$  defining low H-field magnetoresistance according to Eq. (16); curves 1 - 4 are for  $\mathcal{B} = 2, 1, 0.5, 0.1$ , respectively. (b), (c): Total resistance of FET as function on  $\Omega$  for different values of current. (b):  $\mathcal{B} = 1$ , 1 -  $J=0.01$ , 2- 0.05, 3- 0.1, 4 - 0.2, 5 - 0.29. (c):  $\mathcal{B} = 0.1$ , 1 -  $J=0.021$ , 2 - 0.224, 3 - 0.579

$4.6 \times 10^7 \text{ cm/s}$ . We consider properties of the FET at two temperatures:  $77 \text{ K}$  and  $300 \text{ K}$ . For  $77 \text{ K}$  at the mobility  $\mu = 3 \times 10^5 \text{ cm}^2/\text{Vs}$ , we find  $\tau \approx 1.2 \times 10^{-11} \text{ s}$  and  $B = 1$  at  $L_x \approx 5.4 \mu$ . At that the dimensionless cyclotron frequency  $\Omega = 1$  corresponds to the magnetic field  $H = 0.04 \text{ T}$ . The, numerical results presented in Fig. 3 are relevant to these estimates.

For  $300 \text{ K}$  and  $\mu = 800 \text{ cm}^2/\text{Vs}$ , we find  $\tau \approx 3 \times 10^{-13} \text{ s}$ ,  $\Omega = 1$  corresponds to the magnetic field  $H = 1.3 \text{ T}$ . Parameter  $\mathcal{B} = 1$  is realized at  $L_x = 0.14 \mu\text{m}$ . Thus, the results of Fig. 3 are consistent with these estimates for quasi-ballistic FET at room temperature.

The above estimates show that the near-ballistic regime with characteristics presented in Fig. 4 can be realized in GaAs FET with  $L_x = 0.54 \mu\text{m}$  for nitrogen temperature, when  $\mathcal{B} = 0.1$  and  $\Omega'$  corresponds to  $H = 0.04 \text{ T}$ . Similar estimates we found for other III-V compounds.

## VII. CONCLUSIONS

It is known that influence of transverse magnetic field on properties of FET is significant at particular device geometry, when width of the active channel,  $W$ , is much large than its source-to-drain length,  $L$ , and Hall field/voltage is shortened by source and drain contacts, instead Hall currents arise (this can be called quasi-Carbino case). For the *dissipative regime* of electron transport in the channel, the magnetic field effects have been studied in a number of papers (see, for example<sup>12-14</sup>). These studies and their conclusions are correct when electron scattering time is much less than their transit time through the device and, particularly, the drift-diffusion approach<sup>1</sup> can be applied. In the present

paper we analyzed magnetic field effects in FETs with quasi-ballistic and near-ballistic electron transport described by hydrodynamic equations of the Dyakonov-Shur model.<sup>20</sup>

For the considered quasi-ballistic FETs, the main effects of the magnetic field are: significant suppression of currents, increase of saturation voltage, induction of large Hall currents, etc. The density of the Hall currents can exceed densities of the source-drain currents. We found that in quasi-ballistic FETs ( $\mathcal{B}$  is finite) there is no real pinch-off in the channel. Instead, the electric field diverges in the drain side of the device just before the saturation regime.

It is pertinent to note that for the considered geometry of FETs, uniformity of both the equipotential lines and Hall currents in the transverse direction breaks down near the edges of the channel ( $y = \pm W/2$ ), where the current lines exit/enter the source/drain contacts. Thus, to observe predicted above  $J - U$ -characteristics the following condition for the total source-drain current,  $I_{sd}$ , should be fulfilled:  $I_{sd}(U) = J(U)W \gg I_H(U)$  with  $I_H$  been the total Hall current estimated above.

Suppression of currents through the device means increasing resistance. For small magnetic fields, we found general expression for the classical magnetoresistance (proportional to square of the  $H$  field). This expression revealed unexpected result: in nonlinear current regime the magnetoresistance is larger for the devices with higher ballisticity. This property is confirmed by the analysis at high magnetic fields, when the device resistance can raise several times depending on the current.

For near-ballistic transport regime in FETs, the magnetic field cardinally modifies the  $J - U$ -characteristics toward to kink-like behavior. Analysis of such a regime, including the pure-ballistic case, shows that this behavior and strongly nonlinear resistance at almost absent dissipation arise due to pump over electric energy into the Hall currents. We determined regions of voltages, currents and magnetic fields, where these unusual effects occur.

Numerical estimates show that for FETs channels of high mobilities (e.g., low temperature, GaAs) significant effects can be observed in moderate magnetic fields,  $\sim 0.1 T$ . At that, quasi-ballistic regime occurs for a few microns channel length, while for the submicron length the near-ballistic regime can be realized. At moderate mobilities (e.g., room temperature, GaAs), only quasi-ballistic regime can occur and the large magnetic induced effects require the fields  $\sim 1 T$ .

Summarising, we studied semiclassical quasi-ballistic electron transport in short FETs subjected to magnetic field. We determined spatial distributions of electron concentrations, velocities, Hall currents and voltages along the channels. These distributions can be measured by using different scanning probe microscopy techniques. Large Hall currents in the FETs should induce magneto-optical effects, which can be studied in THz spectral range for a single device, as well as for transistor ar-

ray, when the response of the devices is synchronized by the external signal.<sup>26</sup> We defined basic properties of current-voltage characteristics of the FETs in magnetic field, among these we have analyzed kink-like  $J - U$ -characteristic of the near-ballistic device. Peculiarities of magnetoresistance of quasi-ballistic FETs are studied for low and high magnetic fields, and different current regimes. We suggest, that the found results contribute to the physics of short FETs and can be used for developing nanoscale devices for particular applications, including THz emitters/detectors,<sup>13,27-29</sup> magnetic micro sensors, etc.

## ACKNOWLEDGMENTS

This work was conducted in frame of the long-term program of support of the Ukrainian research teams at the Polish Academy of Sciences, project LTP-NAS-KOCHELAP-A7-11-0008.

## AUTHOR DECLARATIONS

Conflict of Interest The authors have no conflicts to disclose.

## DATA AVAILABILITY

The data that support the findings of this study are available from the corresponding author upon reasonable request.

- <sup>1</sup>V. V. Mitin, V. A. Kochelap, M. Stroschio, Quantum Heterostructures for Microelectronics and Optoelectronics, Cambridge University Press, New York, (1999).
- <sup>2</sup>S. M. Komirenko, K. W. Kim, V. A. Kochelap, D. L. Woolard, Low-field electron runaway and spontaneous formation of two-beam velocity distribution in polar semiconductors, Phys. Rev. **B 69**, 233201 (2004).
- <sup>3</sup>Z. S. Gribnikov, N. Z. Vagidov, V. V. Mitin, G. I. Haddad, Ballistic and quasiballistic tunnel transit time oscillators for the terahertz range: Linear admittance. J. Appl. Phys. **93**, 5435 (2003)
- <sup>4</sup>M. Dyakonov and M. S. Shur, Shallow Water Analogy for a Ballistic Field Effect Transistor. New mechanism of Plasma Wave Generation by DC Current, Phys. Rev. Lett. **71**, 2465 (1993).
- <sup>5</sup>M. Dyakonov and M. Shur, Novel terahertz devices using two dimensional electron fluid, IEEE Trans. Electron Devices **43**, 1640 (1996).
- <sup>6</sup>V. A. Kochelap, A. A. Klimov, K. W. Kim, Optical phonon instability induced by high-speed electron transport in nanoscale semiconductor structures. Phys. Rev. **B 73**, 035301 (2006).
- <sup>7</sup>V. A. Kochelap, V. V. Korot'yeyev, Yu. M. Lyashchuk, and K. W. Kim, Nanoscale ballistic diodes made of polar materials for amplification and generation of radiation in the 10 THz-range. J. Appl. Phys. **126**, 085708 (2019).
- <sup>8</sup>K. Natori, Ballistic metal-oxide-semiconductor field effect transistor, J. Appl. Phys., **76**, 4879, (1994).
- <sup>9</sup>J. Wang, M. Lundstrom, Ballistic Transport in High Electron Mobility Transistors. IEEE Trans. Electron Devices **50**, 1604 (2003).

- <sup>10</sup>J. Lusakowski, M. J. Martin Martinez, R. Rengel, T. Gonzalez, R. Tauk, Y. M. Meziani, W. Knap, F. Boeuf, and T. Skotnicki, Quasiballistic transport in nanometer Si metal-oxide-semiconductor field-effect transistors: Experimental and Monte Carlo analysis. *J. Appl. Phys.* **101**, 114511 (2007).
- <sup>11</sup>For example, characterization of electron kinetics by a mobility is not correct for quasi-ballistic transport. Indeed, mobility can be introduced only when scales of spatial nonuniformity well exceeding the mean free path, which is not discussed case. Otherwise, mobility being a local characteristic will be found dependent on device sizes (for example, on the gate length, as in papers<sup>12–14</sup>).
- <sup>12</sup>Y. M. Meziani, J. Lusakowski, W. Knap, N. Dyakonova, F. Teppe, K. Romanjek, M. Ferrier, R. Clerc, G. Ghibaudo, F. Boeuf, T. Skotnicki. Magnetoresistance characterization of nanometer Si metal-oxide-semiconductor transistors, *J. Appl. Phys.* **96**, 5761 (2004).
- <sup>13</sup>N. Dyakonova, F. Teppe, J. Lusakowski, W. Knap, M. Levinshstein, A. P. Dmitriev, M. S. Shur, S. Bollaert, and A. Cappy. Magnetic field effect on the terahertz emission from nanometer InGaAs/AlInAs high electron mobility transistors. *J. Appl. Phys.* **97**, 114313 (2005).
- <sup>14</sup>N. Dyakonova, M. Dyakonov, and Z. D. Kvon, Gated two-dimensional electron gas in magnetic field: Nonlinear versus linear regime. *Phys. Rev.* **B 102**, 205305 (2020).
- <sup>15</sup>G. J. Rees, J. B. Socha, Ballistic electron transport in transverse magnetic field. *Solid State Electronics*, **24**, 695 (1981).
- <sup>16</sup>J. R. Drabble, R. Wolfe, Geometrical effects in transverse magnetoresistance measurements. *J. Electronics and Control*, **3**, 259 (1957).
- <sup>17</sup>Analysis of geometrical effects on the Hall effect and magnetoresistance for different shapes of specimen and positions of current and voltage contacts was done in paper H. H. Jensen, H. Smith, Geometrical effects in measurements of magnetoresistance. *J. Phys. C: Solid State Phys.*, **5**, 2867 (1972).
- <sup>18</sup>N. Dyakonova, M. Dyakonov, and Z. D. Kvon, Gated two-dimensional electron gas in magnetic field: Nonlinear versus linear regime. *Phys. Rev.* **B 102**, 205305 (2020).
- <sup>19</sup>S. M. Sze and K. K. Ng, *Physics of Semiconductor Devices* (John Wiley and Sons, Inc., Hoboken, NJ, 2006).
- <sup>20</sup>M. Dyakonov and M. S. Shur, Shallow Water Analogy for a Ballistic Field Effect Transistor. New mechanism of Plasma Wave Generation by DC Current, *Phys. Rev. Lett.* **71**, 2465 (1993).
- <sup>21</sup>B G Streetman, S K Banerjee, *Solid State Electronic Devices*. Prentice Hall Internationl, Inc. 5-th Edition, 2000.
- <sup>22</sup>Analyzed system of nonlinear equations has also unphysical steady-state solutions, see Ref.[20] and paper: M. Dyakonov and M. Shur, Choking of electron flow: A mechanism of current saturation in field-effect transistors, *Phys. Rev.* **B 51**, 14341 (1995).
- <sup>23</sup>Knap W, Rummyantsev S, Vitiello MS, Coquillat D, Blin S, Dyakonova N, Shur M, Teppe F, Tredicucci A, Nagatsuma T, Nanometer size field effect transistors for terahertz detectors. *Nanotechnology* 2013, 24 (21).
- <sup>24</sup>Ahter N; Pala N, Knap W, Shur M, Terahertz Plasma Field Effect Transistors Detectors, *Fundamentals of Terahertz Devices and Applications*, Wiley & Sons, 2021, 285-322.
- <sup>25</sup>Boubanga-Tombet S, Knap W, Yadav D, Satou A, But DB, Popov VV, Gorbenko IV, Kachorovskii V, Otsuji T, Room-Temperature Amplification of THz Radiation by Grating-Gate Graphene Structures. *Phys Rev X* **10**, 031004 (2020).
- <sup>26</sup>H. O. Condori Quispe, A. Chanana, J. Encomendero, M. Zhu, N. Trometer, A. Nahata, D. Jena, H. Grace Xing, and B. Sensale-Rodriguez, Comparison of unit cell coupling for grating-gate and high electron mobility transistor array THz resonant absorbers. *J. Appl. Phys.* **124**, 093101 (2018).
- <sup>27</sup>Knap W, Rummyantsev S, Vitiello MS, Coquillat D, Blin S, Dyakonova N, Shur M, Teppe F, Tredicucci A, Nagatsuma T, Nanometer size field effect transistors for terahertz detectors. *Nanotechnology* 2013, 24 (21).
- <sup>28</sup>Ahter N; Pala N, Knap W, Shur M, Terahertz Plasma Field Effect Transistors Detectors, *Fundamentals of Terahertz Devices and Applications*, Wiley & Sons, 2021, 285-322.
- <sup>29</sup>Boubanga-Tombet S, Knap W, Yadav D, Satou A, But DB, Popov VV, Gorbenko IV, Kachorovskii V, Otsuji T. Room-Temperature Amplification of THz Radiation by Grating-Gate Graphene Structures. *Phys Rev.* **X 10**, 031004 (2020).